Astron. Astrophys. 339, 173–182 (1998)

ASTRONOMY AND ASTROPHYSICS

N 105 in the Large Magellanic Cloud: a newly evolved H II complex⋆

P. Ambrocio-Cruz[1,2], **A. Laval**[1], **M. Marcelin**[1], **P. Amram**[1], **and F. Comerón**[3]

[1] IGRAP, Observatoire de Marseille, 2, Place Le Verrier, F-13248 Marseille CEDEX 4, France
[2] Instituto de Astronomía, UNAM, Apdo. 70-264, México, D.F., 04510, México
[3] European Southern Observatory, Karl-Schwarzschild-Strasse 2, D-85748 Garching bei München, Germany

Received 4 May 1998 / Accepted 26 June 1998

Abstract. The detailed radial velocity field of the H II region N 105, in the Large Magellanic Cloud, has been obtained for the Hα and [O III]5007 lines with a spatial sampling of 9″ and spectral ones of 16 and 7 km s^{-1} respectively. The line profiles present complex splitting and broadening in several places. The peculiar velocity field and morphology indicate that N 105 contains four bubble shaped nebulae, and two bright distinct quasi spherical H II regions, more or less coeval, embedded inside another large shell nebula. They are formed essentially by the action of the stellar winds of a few exciting stars, born deep inside their parental cloud. This result is deduced from the energy added to the ionized gas by the stellar winds of early type stars and from dynamical simulations combining the effects of stellar winds with those of high density gradients inside the neutral gas. The size and the morphology of the H II region are conditioned by the depth inside the natal cloud; the observed dynamic evolution of the H II region starts at the moment of blow out of the molecular cloud.

The kinematics agrees with the expected results from the stellar content and from the molecular studies. The positions of masers and of an infra-red (IR) source inside N 105 and the structure of this nebula suggest that such an IR source may be the consequence of star formation triggered by the surrounding wind pressure due to the progenitors of the presently evolved stars.

Key words: stars: Wolf-Rayet – ISM: H II regions – ISM: individual objects: N 105 (LMC) – ISM: kinematics and dynamics galaxies: Magellanic Clouds

1. Introduction

Optical (e.g. Conti & Leep 1974) and ultraviolet (e.g. Morton 1967 and Smith 1970) observations show that O stars and supergiants of spectral type earlier than B2 have strong stellar winds with terminal velocities of order $V \simeq 1500 - -3000\,\mathrm{km\,s^{-1}}$ and mass loss rates $\dot{\mathrm{M}}$ approaching $10^{-6}\mathrm{M}_{\odot}\ \mathrm{yr}^{-1}$. Such winds can, over the lifetime of the stars, impart a mechanical energy of the order of 10^{50} erg to the surrounding interstellar medium (ISM), which is comparable to estimates of supernova energy, and an order of magnitude greater than the mechanical energy that might be imparted by expansion of the H II regions.

Since Wolf Rayet (WR) ring nebulae of the Large Magellanic Cloud (LMC) have been observed (e.g. Chu 1982; Rosado 1984 and 1986, Dopita et al. 1994), their large diversity has shown that their progenitors are able to build either a cavity or a circumstellar shell of swept out material, depending on the circumstances of its earlier evolution (Chu 1991). Small ring nebulae (~ 5 pc), recently detected around WR stars (Garnett & Chu 1994; Marston et al. 1994a and b; Marston 1995a), or OB supergiants (Weis et al. 1997) have been confirmed as circumstellar shells of ejecta. On the other hand, a great number of WR stars of the LMC are surrounded by multiple rings or bubbles of a few tens pc, more comparable to the detected IRAS shells (Marston 1995b) which are believed to be interstellar medium swept up by the fast stellar winds of the massive precursors of WR stars.

The WR types are a late stage in the evolution of massive stars; their actions on the ISM at scale of a few pc, deal with a medium where the kinematics has been already transformed by previous phases of stars. Furthermore, as the WR stars commonly belong to rich OB associations, the structure of the ionized medium which encircles the massive stars, is undoubtedly relevant to a combination of all their interactions with the environment. The proper dynamical action at the WR phase is not always clear.

The dynamics of some ionized shells, as N 57c or N 79 west (DEM 6 North) have already been studied in detail (Chu 1982; Rosado 1984). In this work we study the nebula N 105 (DEML86, B051012-6857, new IAU nomenclature), for the purpose of examining an interaction of massive stars with the environment in a case where the nature of their interactions is merely discerned. Using kinematics and dynamics of the ionized gas, we expect to disentangle the observed motions, and to discriminate their origin.

Other reasons have also led to such a choice: a loose cluster (NGC 1858) with an OB association (LH31) is embedded in the nebula. Other features provide evidence for a site of recent star formation, such as an IR source and OH and H_2O masers. More-

Send offprint requests to: P. Ambrocio-Cruz
Present address: IGRAP, Observatoire de Marseille, 2, Place Leverrier, F-13248 Marseille CEDEX 4, France

⋆ Based on observations done at La Silla (ESO)

over the nebula N 103 (B050905-6849 or DEML84, Ambrocio-Cruz et al. 1997), is at a projected distance of only 3'.5 to the north-west, which is ~ 50 pc assuming a distance modulus of 18.5 mag of the LMC (Feast 1991; Panagia et al. 1991; Madore & Freeman 1998). Embedded in N 103 are an old cluster (N GC1850A, ∼70Myr old) and a young cluster (NGC 1850B, ∼6Myr old), which yields the ionizing flux. N 103 does not show any sign of very recent star formation, and presents the rare opportunity of being linked to two supernova remnants (SNRs). N 103 presents a low-level excitation, while N 105 is highly excited, displaying a bright [O III] emission. What can be the similarities and the differences between N 103 and N 105? Did they proceed from similar star formation scenarios?

In this publication we present some answers to such inquiries, using the results of Hα and [O III]5007 observations performed with a scanning Fabry-Perot interferometer attached to the 36 cm telescope in the European Southern Observatory of La Silla and operated under the same conditions as the observations of the H II region N 103 described by Ambrocio-Cruz et al. (1997). In summary, we obtain monochromatic images limited by interferential filters of ∼12Å wavelength band, and spectral information in a field of view of $38' \times 38'$, and an angular sampling of $9''$, the spectral sampling being 16 kms^{-1} for Hα line and 7 kms^{-1} for [O III] line.

In the next section, we present the local environment of N 105 as well as the distribution of stars inside the nebula. Sect. 3 describes the kinematic field. In Sect. 4 the physical parameters of each observed region are given. Finally, Sect. 5 is devoted to a discussion of the results.

2. Stellar characteristics and local environment of the H II region N 105

2.1. Stellar content

The H II region N 105 (Henize 1956), B051012-6857 or DEML86 (Davies et al. 1976), hereafter N 105, is situated at the western side of the bar of the LMC. The cluster NGC 1854-1855 is located at the north-western edge of the nebula, $4'$ (58 pc) from the center. Freeman et al. (1983) have studied this cluster, finding an average heliocentric velocity of 242 ± 9 km s^{-1}. The age of the cluster NGC 1854-55 is estimated in the range from 22 Myr (Alcaino & Liller 1986) to 40 Myr (Cassatella et al. 1996). From Santos et al. 1995, this cluster is not related with N 105 because they are not coeval, moreover we will show in Sect. 3 that the systemic velocity of N 105 is different from the average velocity of this cluster. NGC 1858 is a younger sparse cluster embedded in the H II region N 105. Alcaino & Liller (1986) have determined an age of 17 Myr, and Vallenari et al. (1994), from UBV Johnson CCD photometry, have given an age of 8 Myr for this loose cluster.

Involved in NGC 1858 is the OB association LH31 (Lucke & Hodge 1970), having 18 OB stars, two Wolf-Rayet stars (Br16 and Br16a, of spectral type WN3-4+OB and WC5+O respectively, Dopita et al. 1994), and a diffuse faint X-ray emission probably originating inside the association (Wang & Helfand 1991 and Chu 1997). Dopita et al. (1994) found a faint filamentary nebula $52'' \times 64''$ (13pc×16pc) appearing only in [O III], associated with the star Br16 and a ring nebula of $18''$ (4pc) in diameter associated with Br16a. Koesterke et al. (1991) have carried out a spectral analysis of the WR star Br16, they determined a temperature $T_* = 50000$ K, a terminal velocity $V_\infty = 2650$ km s^{-1} and a mass loss rate $\dot{M} = 8 \times 10^{-5}$ M$_\odot$ yr^{-1}.

Alcaino & Liller (1987) and Vallenari et al. (1994) performed photometry of the clusters. The colour excess of N 105 has been deduced by Caplan & Deharveng (1985, 1986) on the basis of Hα and Hβ photometry as $E_{(B-V)}$=0.15. The isochrone fitting by Alcaino & Liller gives $E_{(B-V)}$=0.15 too. Hereafter we assume $E_{(B-V)}$=0.15. It is obvious from the V image (Vallenari et al., 1994), from R photographs (Alcaino & Liller, 1986 and Morgan & Good 1985), and from our Hα and [O III] images that the bright parts of N 105 are surrounding a very faint emission zone. However, since a few faint stars can be seen through this area from R photographs, the faint emission area is due to a localized presence of dust.

As the observed extinction cannot be explained from the HI column density with an assumption of a normal hydrogen to dust mixture (Caplan & Deharveng, 1986), N 105 falls in the group of H II regions presenting the most extreme failure. It seems that a significant part of the dust is located within (or just in front of) the emitting gas. This assumption is also suggested by an observed molecular cloud located at the position of the fainter optical emission nebula (see next section).

In the following, star names are those of Alcaino & Liller (1987).

2.2. Environment and ionized gas morphology

The thermal radio continuum source MC 23 (McGee et al. 1972) or B0510-6857 is associated with the optical nebula N 105. McGee et al. (1974), from H109α recombination line observations made in the direction of N 105 have calculated a radial velocity of 254 km s^{-1}. MC23 is associated with a water vapour maser at heliocentric velocity of 253 km s^{-1} (Scalise & Braz 1982), confirmed by Whiteoak et al. (1983) at 257 km s^{-1}. Haynes & Caswell (1981) have reported the OH counterpart of this H_2O maser, with heliocentric velocity of 254 km s^{-1}. Israel et al. (1993) have detected a ^{12}CO cloud at the same position as the H_2O maser with a heliocentric velocity of 256 km s^{-1}. More recently, Chin et al. (1997) have detected a ^{13}CO core with a diameter of $66''$ (16 pc) and a heliocentric velocity of 256 km s^{-1} at the same position.

All these molecular velocities agree perfectly also with the HI low velocity layer (258 km s^{-1}) detected by Rohlfs et al. (1984).

Epchtein et al. (1984), from IR observations have detected a protostar at the same position as the H_2O maser. Protostars and masers are strong indications that some star formation should still be active there.

The dimensions of N 105, derived from the Hα emission (Fig. 1) are $8'.1 \times 7'.2$ (118pc×105pc). Contrary to N 103 and to many bubble like nebulae of the LMC of similar size, the morphology is made of many smaller bubbles or nebular intri-

cate filaments, and bright entities (Figs. 1a and 1c). The Hα and the [O III] morphologies are unlike, showing that these small nebulae and bright entities must be influenced either by the UV flux of the ionizing stars, or by dust clouds.

Since many massive stars exist in LH31, loops and bubble shapes are not surprising; however their positions look unexpected, specially regarding the WR stars.

We identify every one of these several apparent bubbles by adopting the Henize number followed by a letter indicating their position in the nebula (Fig. 1a). Two bright entities (BE) denser than the bubbles (Fig. 1a), hereafter called NBE for the northern one and SBE for the southern one, divide the other smaller bubbles, while a large diffuse external Hα and [O III] shell (hereafter called N 105L), envelopes the whole complex. N 105W looks to be cut to the North by the nebula N 105NW and superimposed to the South with N 105SW (Fig. 2b), but they may be situated in different planes. N 105SW is limited toward the East by the ionization front of the SBE. A comparison between the Hα and [O III] photographs by Dopita et al. (1994), completed by Figs. 1a and 1c, inclines to think that the regions of high excitation are, by decreasing order, N 105W, NW and SW, and the BEs, while N 105NE is conspicuous in the Hα photograph by Dopita et al. (1994) and that the Eastern side of the external shell N 105L is hardly seen in [O III] emission (Fig. 1c).

The division into two parts, NBE and SBE (Fig. 1b), may be an illusion, since the OH and H_20 masers are detected in the same area which contains also the radio continuum emission peak. Thus, the apparent optical emission void, already mentioned in Sect. 2.1, is likely due to the presence of dust. The ^{13}CO cloud detected by Chin et al. (1997) is seen centered on this void and has almost the same dimension (66″ $\sim$16 pc).

The bubble N 103 is the result of a SN explosion (Ambrocio-Cruz et al. 1997; Milne et al. 1980). However an assumption of quasi-simultaneous explosions of supernovae to explain the four small bubbles of N 105 is inappropriate at such small spatial scale. Then the most obvious process able to create several quasi spherical disjoined bubbles, is the wind pressure of dispersed massive stars, inside a homogeneous ISM.

2.3. Blue stars inside the nebulae

2.3.1. Blue stars associated with the bubbles

The association LH31 is mainly embedded inside the BEs. Then other blue stars nearer to the small bubbles are examined (Fig. 1). They are presented in Table 1, to which are added two stars situated in the outermost part of the cluster NGC 1854-55 (stars No. 63 and 174), assuming that they are at the same distance as LH31. Indicative spectral types were derived from Alcaino & Liller's (1986) photometry with the calibration of Schmidt-Kaler (1983) ($E_{(B-V)} = 0.15$ mag., see Sect. 2.1). But the derived spectral types are bluer if the extinction is higher than 0.15. The spectral type of the star No. 61 (Sk -68°59 or HDE 269116) was taken from the spectroscopic study of Walborn (1977); it is nearly the same as the one derived from photometry (B0Ia).

From Panagia's (1973), Vacca et al.' (1996) and Barlow et al.' (1981) tabulations of Lyman photon luminosities, we have calculated an ionizing flux of $3.9 \pm 2.3 \times 10^{49}$ph s^{-1} for these brighter stars inside N 105. Such a flux is smaller than those evaluated from our Hα luminosity of the whole nebula ($1.5 \pm 0.9 \times 10^{50}$ ph s^{-1}). So, N 105 is not predominantly photoionized. Since the deduced spectral types indicate potentially exciting stars with very different effective temperatures, the excitation level of the nebulae can help to discern true links. It can be estimated by the $\{$[O III]/H$\beta\}$ ratio of the ionized gas, derived from our [O III]5007 observations. This estimated ratio is related to the true [O III]/Hβ ratio by a factor which is the ratio of the respective transmissions of the interferential filters.

The WN star Br 16, is at the very edge of the stellar association LH31, to the West and inside N 105W. The estimated value $\{$[O III]/H$\beta\}$ (Table 2), confirms a high-level excitation of N 105W, and thus its ionization by Br16 is very likely.

On the other hand, the WC star Br 16a is situated close to N 105NE. However, [O III]5007 is below our detection limit for this bubble (see Sect. 2.2). Therefore the WC star might not participate to the ionization of the gas of N 105NE, and their apparent vicinity is probably a projection effect. Two or three other moderately blue stars are seen at the periphery of the NBE; it is questionable whether they participate to the ionization of N 105NE or not.

In N 105NW, most of the excitation can be provided by the star No. 63 only, seen at the periphery of NGC 1854. In N 105SW, the presence of the star No. 61 (NGC 1858) can easily explain the observed excitation; some other less massive stars are present too. Therefore the presence of blue stars and the excitation levels of the small nebulae are strong arguments in favor of actually different bubbles.

2.3.2. Exciting stars associated with the Bright Entities (BEs)

The WC star Br16a is seen embedded inside the NBE. The $\{$[O III]/H$\beta\}$ value of the NBE (1.15) is the highest (Table 2), confirming the link of the NBE with the WC star Br16a. The other WN star Br16 is also seen projected at the edge of the NBE, although not embedded as deep as the WC star. The $\{$[O III]/H$\beta\}$ value (0.52) of the SBE is lower than the value of the NBE. It shows that the WR stars are not the ionizing agents of the SBE.

Using the total luminosity function established by Vallenari et al. (1994) for NGC 1858, it turns out from the Initial mass function (IMF) that at least one star has been more massive than 60 $M_\odot$ and four stars between 40 and 60 $M_\odot$. The most massive ones must be observed as the most evolved stars, such as the two WR stars. It agrees with the blue stars observed by Alcaino & Liller (1987). It agrees also with the ability of one or several stars to ionize the oxygen into O^{++} in the SBE.

Anyhow it is not obvious whether the two BEs are distinct nebulae (Sect. 2.2). For instance the CO cloud could inhibit the UV flux of the WC star to extend to the southern gas.

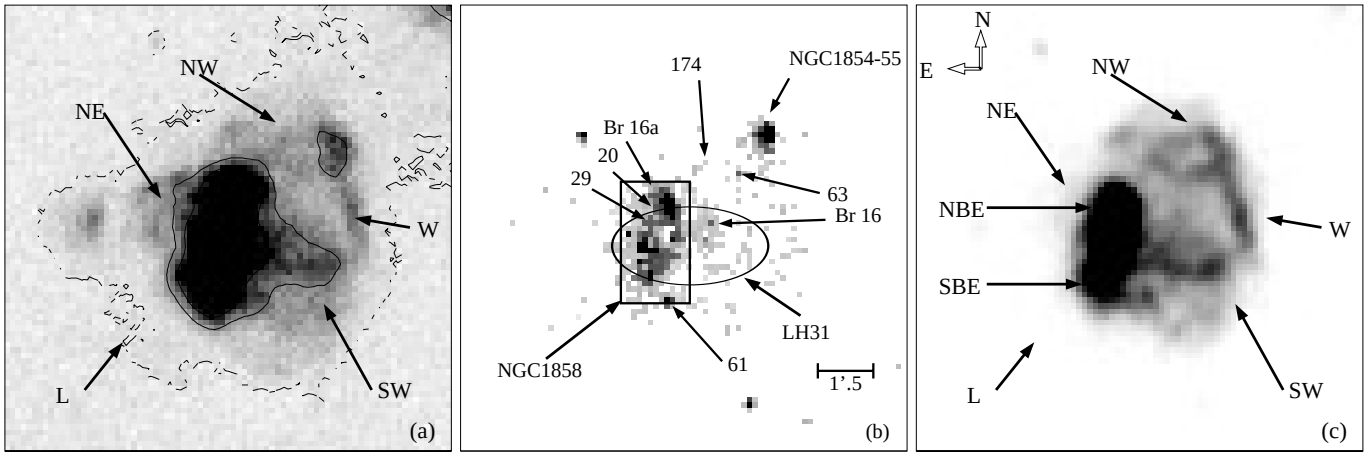

Fig. 1a–c. Monochromatic maps of N 105. The scale is the same for each map. **a** Hα emission exhibiting the several nebulae forming N 105. **b** Continuum emission associated to Hα with the position of the most luminous blue stars of the stellar association and the stellar clusters. **c** [O III]5007 emission.

Table 1. Parameters of candidate stars

Star	M_v	(Deduced) Sp. Type	V_∞ (km s^{-1})	$\dot{M}$ (10^{-5}M$_\odot$yr^{-1})	L (10^{36}erg s^{-1})	Associated nebula
(1)	(2)	(3)	(4)	(5)	(6)	(7)
Br16 *	–	WN3-4+OB	2650	8	100	N 105W
Br 16a	–	WC5+O	2800 **	3	70	BE
61	−6.9	BO.7Ia	1700	0.3	1	N 105SW
20	−3.7	(B1IV)	–	–	~ 0.01	N 105NE
28	−4.6	(O8.5V)	–	–	~ 0.5	N 105E
29	−4.5	(O9V)	1700	0.03	0.3	N 105NE
174	−2.5	(B2)	1000	~ 0.01	0.01	N 105NW
63	−5.2	(O7V)	2000	0.06	1	N 105NW

Notes:
(1) Star's number from Alcaino & Liller (1987).
* Data for this star were measured by Koesterke et al. (1991).
(2) Visual absolute Magnitude.
(3) The spectral types deduced from photometry are shown inside ().
(4) Terminal velocity of stellar wind deduced from Walborn et al.' (1995) parameters of massive stars.
** Value deduced from Conti & Underhill' (1988) calibrations.
(5) Mass-loss rate from Conti & Underhill' (1988) and Lamers' (1981) calibrations.
(6) Mechanical luminosity of the stellar wind.
(7) Associated nebula.

Why is Br 16a embedded in such a BE instead of a bubble, which is expected from the action of its massive progenitor? Dopita et al. (1994) have detected a small and bright ring nebula of 18″ of diameter (4 pc) surrounding the WC star which was probably blown by its own wind; nevertheless it is not seen at our spatial resolution.

3. The kinematic field

Spherical expanding motions inside a bubble lead to obtain the classical distribution of single profiles at the periphery, and splittings in the inner gas. On the contrary splittings at the periphery can appear with other types of motion such as "champagne effect" (e.g. Yorke et al. 1982; Comeron 1997) or with second generation exciting stars (e.g. Rosado et al. 1996, 1998). Considering the maps of the small bubbles, the observed pattern is complex. Fig. 3 illustrates some examples of the radial velocity profiles across the nebula. They are fitted with Gaussians convolved by the instrumental function. The radial velocities given hereafter are heliocentric. Along the edges the [O III] line widths are often broad, the FWHM reaching 14 or 16 kms^{-1}. At a few places of the rim, the filament breaks off, and the smooth faint emission presents there splittings, showing the gas flowing out.

The velocity components are different inside each of the small regions (N 105W, SW, NE, NW and L). The distribution

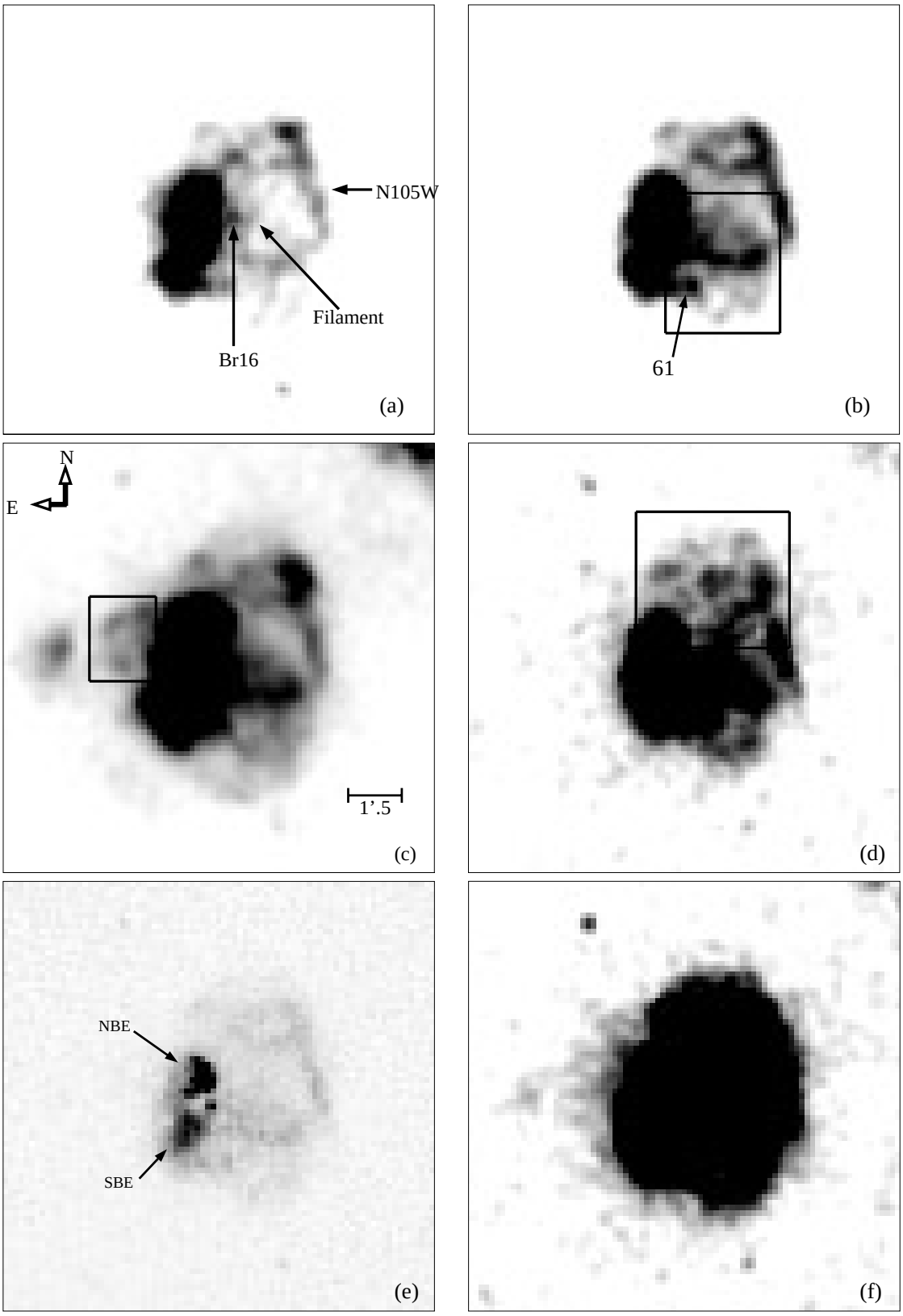

Fig. 2a–f. Monochromatic images showing the several nebulae forming N 105. The scale is the same for each map. The intensity scale is fitted for each small bubble to be visible at best. **a** [O III] image illustrating the bubble like morphology of N 105W, the position of WR star Br16; a faint filament is marked. **b** [O III] image of N 105. The square shows N 105SW nebula and the arrow points to the position of the OB star No. 61. **c** Hα image. The square shows N 105NE. **d** [O III] image of N 105, with the bubble-like nebula N 105NW. **e** and **f** [O III] images exhibiting the nebula N 105L. The arrow in **e** shows the two BEs separated by a void, and **f** displays the most external filamentary part of N 105L.

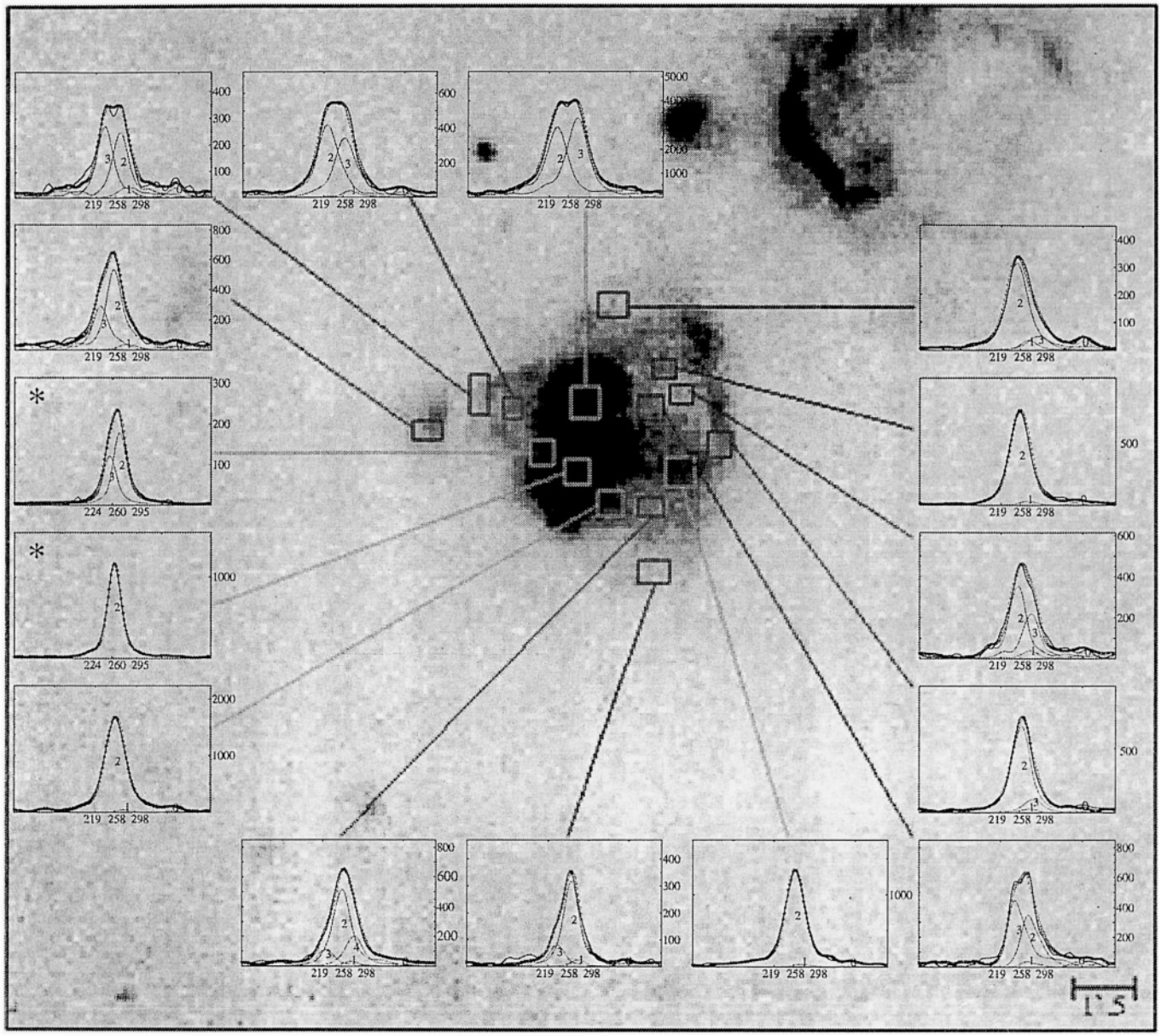

Fig. 3. Some examples of the Hα radial velocity profiles and their location across the nebula. The x-coordinates in the profiles give the radial velocity in km s^{-1} and y-coordinates give the intensity of line in arbitrary units. Profiles marked with * are [O III] radial velocity profiles. No. 0 and 1 profiles are night-sky lines. The dotted profile is the sum of all profiles. The nebula in the upper right corner is N 103.

of the splittings and of the single profiles along the intense filaments confirm that the small apparent bubbles do not overlap.

The BEs behave differently. Single profiles fit the inner part of the SBE, with a maximum of density in the center; splittings are mostly located at the edges of the SBE. The brightness of the SBE decreases from north to south, being brighter near the apparent optical emission void between the two BEs. In the NBE, the brightness is the highest near the WC star Br16a. The brightest peak occurs inside 9″ (2 pc), and it is not resolved at our spatial resolution. The [O III] emission of the surrounding gas exhibits enlarged line profiles, broader towards the northern periphery and splitted around the WC star.

Table 2 gives a summary of the main characteristics of all the nebulae forming N 105. We give the dimension of each region, which is the same in Hα and [O III] emissions except for N 105NE where the [O III] emission is very weak, and N 105NW which is best seen in the [O III] line (Fig. 2d). The Hα surface brightness ($S_{H\alpha}$) was calculated in the same way as for N 103 (Ambrocio-Cruz et al. 1997) and corrected for interstellar extinction (Sect. 2). The inherent uncertainties have been estimated (Ambrocio-Cruz et al. 1997); when the total flux of the H II region has been determined by Caplan & Deharveng (1985), they are about 35% for the fluxes in Table 2.

In Table 2 we have also quoted kinematic quantities obtained from our data such as: heliocentric systemic velocity (V_s) and expansion velocity (V_e) for the complex velocity profiles. These quantities are difficult to evaluate inside rich stellar fields (Chu 1991); hereafter they have been deduced from splitting near the geometrical center and not from the extreme velocities because the signal/noise ratio of these extreme velocity components is very low and the splittings in the more external zones of the regions can be due to shell instabilities (Garcia-Segura et al. 1996; see also the discussion in Sect. 5).

We have also estimated the dynamic timescale t (in units of 10^6 years) of the nebulae defined as $t_6 = 0.59\frac{R}{V}$ (Weaver et al. 1977).

4. Comparison of wind driven bubble models and of the observations

In order to explain the motions in each of the nebulae forming N 105, we have first applied the time-depending model of a stellar wind driven bubble of Weaver et al. (1977). Such a modelized bubble of radius R (in pc) and expansion velocity V_e (in km s^{-1}) requires a wind power L (in unities of 10^{36} erg s^{-1}), which is given by: $L = 3.35 \times 10^{-7} R^2 n_o V^3$

This pre-shock density, n_o, can be calculated by assuming an isothermal shock and a spherical shell of radius R and thickness ΔR. The parameter ΔR is classicaly evaluated by assuming that the mass in the shell is the same as the mass swept away in the sphere of radius R with density n_o. Then it enables the pre-shock density, n_o (in cm^{-3}), to be estimated from the shock radiated Hα surface brightness $S_{H\alpha}$, the radius R (in pc) of the bubble and the shock velocity V_e, according to the following relation: $n_o = \sqrt{\frac{S_{H\alpha} C^2}{5.85\times10^{-8} R V_e^2}}$ where C is the sound velocity in the interstellar medium (we have adopted 10 km s^{-1}).

Table 3 gives the values of the rms electron density, $< n_e >$, n_o and the required wind power L to drive each bubble, using the observed values of Table 2. The rms electron density of the H II region has been evaluated under the assumption of an homogeneous sphere of radius R. The values obtained for the quantity L (Table 3) fall in the range expected for wind power driving bubbles; therefore stars alone are believed to supply the energetic amount. However the mechanical luminosity of the stellar winds listed in Table 1 either just fits with, or is smaller than the required wind power (Table 3) except for N 105W. The kinetic efficiency, usually taken between 1% and 20% (Chu 1982 and Van Buren 1986), makes the discrepancy worse.

We conclude therefore that the local conditions do not match Weaver's model. Several obvious departures have already been stressed by Oey (1996) who has discussed similar discrepancies between Weaver's model and observations, and shown that, because the stellar evolution has transformed the local medium, it results that either observed expansion velocities or bubble radii, are larger than expected.

Prior to that evolution, the probable proximity of the relics of the initial molecular cloud suggests that density gradients may also have caused a different nebular evolution, as studied by Yorke et al. (1982) and recently Comerón (1997). Their "champagne" phase is a supersonic expansion of the ionized gas promoted by the negative density gradient. Such an effect is still enhanced by the stellar winds of massive stars, because the mechanical power contained in the wind can be efficiently transferred to the surrounding gas (Dyson & Williams 1980).

Later on, when the star evolves towards the WR stage, the evolution phases of its circumstellar material has been modelled by Garcia-Segura et al. (1996a,b). The new WR star illuminates the envelope lost during the RSG or LBV and makes it expand.

At which evolutionary stage do we observe the apparent bubbles of N 105?

4.1. N 105W

The [O III] ionization front of N 105W (Fig. 2a) is well separated from the strong emission of the BEs. The WN star Br16 is embedded close to the eastern boundary of N 105W, 1' (15 pc) from the center of the bubble, and linked to this center by a noteworthy filament. The profiles in direction of Br16 and in its neighborhood show splittings. On the other hand the energy involved in the bubble is lower than the mechanical luminosity of the stellar wind of Br 16, derived from the data of Koesterke et al. (1991).

From spectral analysis of Koesterke et al. (1991) the progenitor of Br16 was a star of 40 $M_\odot$. It agrees with Maeder's (1996) models for a metallicity Z=0.008, showing that only stars more massive than 40 $M_\odot$, can reach the WR phase, with a lifespan of the WR stage of $\sim 10^5$ years.

4.2. N 105SW and N 105NW

N 105SW is the faintest of the five nebulae, nevertheless it can be seen at both Hα and [O III] emission (Fig. 2). N 105SW is superposed to the southern side of N 105W. The star No 61 is localized to the eastern side of N 105SW; for a bolometric magnitude of this star of -9.5 (Ardeberg & Maurice, 1980), a effective temperature of 25000 K and a metallicity of 0.008, the initial mass deduced from the models of Schaerer et al. (1993) is 40 $M_\odot$. Although the wind of such stars can yield the required power, the location of the splittings regarding to the star is not satisfactory because the line profiles at both Hα and [O III] emission are single in the direction of this star, but splitted in the center of the nebula. Even if the action of the wind of this star is not reliable with the double component, its UV flux may contribute to the local ionization.

N 105NW is best seen in [O III] line, showing a ring shaped nebula. The derived spectral type of the central stars No. 172, 173 and 174 (Alcaino & Liller 1987), is B2, which does not agree neither with the high level of excitation nor with the energetic input in the gas. In the south-western boundary of the nebula lies an O7V spectral type star (No. 63 of Table 1), nearer to the cluster NGC 1854. The line profile in the direction of this star shows splitting at both Hα and [O III] emission. Applying the stellar wind model (Table 3), the energetic input in N 105NW would thus require at least the presence of an O star

Table 2. Physical parameters of the observed regions

Region	Radius (pc)	{[O III]/Hβ}	$S_{H\alpha}$ (1) (erg cm^{-2}s^{-1}sr^{-1})	V_s (2) (km s^{-1})	V_e (3) (km s^{-1})	t 10^6 yr
H II Region	56		3×10^{-5}	255	–	–
N 105 W	22	0.92	5×10^{-5}	267	23	0.6 ± 0.1
N 105 SW	20	0.43	2×10^{-5}	275	14	0.8 ± 0.3
N 105 NE	14	0.07	3×10^{-5}	246	22	0.4 ± 0.1
N 105 NW	20	0.95	4×10^{-5}	263	13	0.9 ± 0.3
NBE	8.5	1.15	57×10^{-5}	264	–	–
SBE	8.5	0.52	55×10^{-5}	262	–	–

Notes:

(1) Hα flux corrected for interstellar extinction.
(2) The accuracy of these determinations at S/N ratio > 4, is $\pm$ 4 km s^{-1}.[(3)] The FWHM of the line profiles are in the range 12–16 km s^{-1}.

Table 3. Main characteristics of the nebulae (bubbles)

Region	$< n_e >$ (cm^{-3})	n_o (cm^{-3})	L (10^{36}erg s^{-1})
H II Region	2	–	–
N 105 W	14	3	6 ± 4.8
N 105 SW	6	3	1 ± 0.8
N 105 NE	13	3	2 ± 1.6
N 105 NW	8	4	1 ± 0.8

which might be the star No. 63, if it is actually at the same distance as NGC 1858. According to the stellar population in this region, N 105NW may also be the ring nebula of the precursor of another evolved star. Spectroscopic observations of the stars located in this region have to be encouraged in order to precise the progenitor.

4.3. N 105NE and N 105L

The value of velocities of N 105E were obtained from Hα emission profiles only. Let us note the lower systemic velocity (Table 2). The profiles across the center of N 105NE, in the west-east direction, show the largest splittings in this bubble. However they are characterized by a blueshifted velocity component, at 230-240 km s^{-1}; the wind power of OB stars No. 20 and No. 29 cannot provide for such an input of kinetic energy, so may it be Br16a that blows N 105NE despite of its lack of [O III] emission? The undetected [O III] emission and the bluer "systemic" velocity incline to think that a strong obscuration in this part of N 105 masks the gas layers at the rear.

N 105L is not a bubble, but the most external shell, seen at the very southern border to the east, referred to as DEML87. At some places it is barely visible in the [O III] line. As in N 105NE, the kinematic field often presents a faint blueshifted velocity component, $\sim$ 236 km s^{-1}, and the main component still at 260 km s^{-1}. The faint component could be an extension (towards the south and towards the bluer velocity) of the blueshifted component of the BE. Such a component is not found elsewhere in the vicinity, specially toward the nebula N 103. Therefore the origin of the blueshifted component does not seem likely to be another distinct ionized slab. It is possible that the large shell N 105L, which has the same size and systemic velocity as the H II region (Table 2), originates in an interstellar bubble blown up by the OB association LH31. Moreover, from UV studies, Smith et al. (1987) have determined a Lyman flux

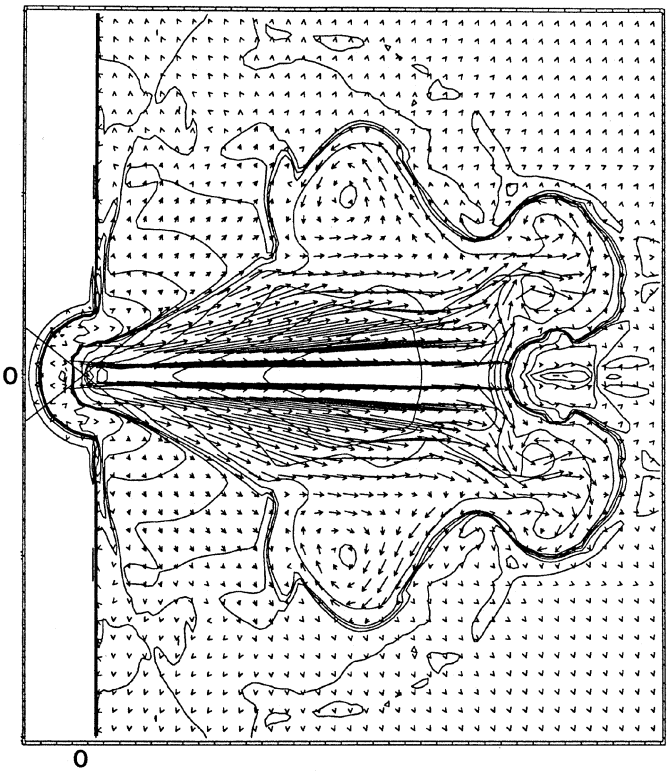

Fig. 4. Simulation of the evolution of the velocity (represented by arrows) superposed to the contour of density for the gas surrounding a O9V star (see text) located 1.5 Strömgren radii from the cloud boundary. The frame corresponds to the evolution time 3.25×10^5 yr after the blow out, the size of the square frame is 14.3 pc. The star's location is at (0,0).

of 9.17×10^{49} ph s^{-1} for LH31, while our Hα observations suggest $N_{\rm Lym} = 1 \pm 0.6 \times 10^{49}$ph s^{-1} from the BEs. Thus N 105L may have been ionized by the excess of UV flux of LH31 running away from the BEs. On the other hand there is a diffuse X-ray emission of 4' (58 pc) in dimension (Wang & Helfand 1991) centered on the OB association, with a fainter emission extending to 6' (87 pc) (Chu 1997). Wang and Helfand propose that a SNR hitting the dense shell of a young bubble may produce such enhanced X-ray emission. Perhaps N 105L and its blueshifted velocity component might be the most likely bubble to relate to such an event. But another explanation could be wind-driven bubble evolving in a dense medium.

It is not clear whether N 105NE may be part of N 105L.

Therefore none of N 105W, SW, NW and NE can be explained only as stellar wind driven bubble of in-situ stars, inside an homogeneous ambient medium. Scenarii of evolution within high gradient densities have to be examined (see Sect. 5).

4.4. The Bright Entities (BEs)

No shell structure is visible on the [O III] images of these bright quasi spherical entities denser than the bubbles (Fig. 2e). The splitting in the profiles of the NBE can be explained by the existence of the WC star Br 16a (Tables 1 and 3), which is embedded inside a zone where the profiles show clear splitting. The intensity of the two velocity components decreases outward, mainly in [O III] emission. It is actually surprising that no bubble is seen associated with the progenitor of Br 16a, which is the only star able to explain the excitation of the NBE. The precursors of WC stars usually drive powerful winds which should have already transformed the environment.

Thus it seems likely that ISM density conditions dictate the observed morphology near the WR stars. The localization of the CO cloud between the association LH31 and the WC star can explain why we do not see any bubble associated with the WR star precursor: the molecular cloud, exposed to the UV flux, is still being evaporated and ionized. Its matter can be seen filling up the available volume and also confined there by the surrounding stellar winds.

The SBE may also have the same origin, since the UV flux of the stellar association LH31 is operative and slightly less efficient.

5. Discussion

N 105 consists of two BEs, four smaller bubble shaped nebulae of similar dimensions, and a large external shell. The bubbles were formed by the action of the stellar winds of a few very massive stars. The luminosity of these bubbles fall in the range expected for wind power driven bubbles. However, the mechanical luminosity of the stellar winds of individual stars is smaller than the required wind power, so the local conditions do not match Weaver's model. Therefore the initial conditions in N 105, especially the density, must be different. All the nebulae first evolve inside ambient density gradients; usually these gradients decrease, and ionization renders the medium homogeneous before the stars evolve. The difference presented by N 105 is that, despite the ages of its ionizing stars, it has not disrupted its whole parental molecular cloud, and is still evaporating the clouds in an inhomogeneous medium. The eccentric location in their bubble of the stars Br16, Br16a, and No. 61, close to the location of the observed molecular cloud, supports the hypothesis of blisters of the apparent bubbles.

Fig. 4 shows a simulation of the evolution of the velocity for the gas surrounding a O9V star located 1.5 Strömgren radii from the cloud boundary ($n_{\rm H}$=10^4 cm^{-3}), with stellar parameters of T$_{eff}$=36,000 K, $\log N_{\rm Lym} = 48.56$ and $\dot{\rm M}$=3 $\times$ 10^{-7}M$_\odot$/yr. The frame corresponds to the evolution time 3.25×10^5 yr and the computational grid size is 14.3 pc. Details of numerical method can be found in Comerón (1997). Fig. 4 shows that several spherical features appear, where the different directions of velocity will appear as line splitting. The greatest expansion of the gas occurs along the axis passing through the star and the center of the bubble. Such a pattern can match the small bubbles, but not the BEs. In the bubble N 105W the highest motions are indeed found along the already noted filament, which is 45″ (11 pc) long to the west of the WN star Br16. Gas concentrations occur along the filament, in the middle of the whole structure, so the density decreases outwards. In such a scenario the progenitor of the WN star Br16 would have been the source of energy for all the western side; the stars mentioned in Table 1 may play only a secondary role, if they are actually at the same distance as the bubbles. The only difference is that it should have been at least an O7V star, in order to be massive enough to evolve through a WR phase.

In almost all the nebulae forming N 105, the putative exciting star is localized at the boundaries of its associated nebula, nearly in the shell, as expected from the simulations (Fig. 4). Perhaps all these bubbles were formed by stars of Table 1 located near the boundary of their parental molecular cloud. In this case it may have been the same cloud whose gradient density allowed the gas velocity to grow and the wind driven bubbles to expand.

The features of the eastern part of N 105 (BEs, N 105E, N 105L) are likewise consistent with a location nearer to the core of the molecular cloud. The ionized environment of the WC star Br16a still requires a source of matter to be evaporated. The virial mass estimated from the observed molecular cloud is still large: 10^5 solar masses in a 16 pc diameter area (Chin et al. 1997).

H_2O masers are located near the eastern boundary of N 105W at the very edge of the NBE, close to the probable IR protostar. H_2O masers are known to exist during low mass star formation, which suggests that star formation is still going on in the core of N 105, between 40″ to 60″ (10 to 14 pc) from the most evolved stars in the field. On the other hand, a strong [O III] emission peaks near the same area, 30″ (7 pc) north of the WC star Br16a. Its morphology strongly suggests a compact H II region, but its ionization source could be either the WR stars or a star still hidden within. Unlike N 105, no maser is detected in N 103 and only a ^{12}CO molecular cloud, probably small and/or faint (Israel et al. 1993), is known in the direction of DEM85 (to the east of N 103). N 103 presents a very faint

[O III] emission, which implies a lack of very massive stars, and is associated with two supernova remnants.

Which mechanisms can initiate the collapse of the cloud leading to a new generation of stars? An origin from a SN explosion is often suspected; but in the case of N 105 compressions of the gas are more likely to be caused by shocks produced during the wind interaction with the ISM. The simulations show instabilities developing around the wind blown structure and increasing with time. The shock wave produced by the winds of the progenitors of the WR stars may have triggered the new star formation on some part of the CO cloud, whose remaining part is still gravitationally bound (Chin et al. 1997). Moreover the location of the masers and protostar suggests that the molecular gas is confined by the stellar winds of the WR stars and of the association LH31.

Conclusion

N 105 is an H II region with complex morphology and kinematics of small bubbles and bright quasi-spherical regions. It has been formed by the action of the most powerful winds of its exciting stars, enhanced by their birthplace being deep inside the parental cloud, which led the H II regions to evolve as blisters. The observed difference of evolutionary stage between the nebulae N 103 and N 105 may arise from a different mass of the original cloud or from the stars of N 105 being embedded deeper within their initial cloud.

The nebulae N 103 and N 105 are the most westerly of the five bubble shaped nebulae spread further the bar of the LMC. The evolutionary stage and more detailed simulations fitted to each particular case (N 105, N 119 and N 113) will be presented in a forthcoming paper.

Acknowledgements. P. Ambrocio-Cruz wishes to thank DGAPA-UNAM for financial support. We are grateful to Dr M. Rosado for valuable comments and encouragement. We acknowledge Dr Y.H. Chu for fruitful comments.

References

Alcaino G., Liller W., 1986, Mem. Soc. Astr. Ital., 57, 491
Alcaino G., Liller W., 1987, AJ 94, 372
Ambrocio-Cruz P., Laval A., Marcelin M., Amram Ph., 1997, A&A, 319, 973
Ardeberg A., Maurice E., 1980, A&A 91 53
Barlow M.J., Smith L.J., Willis A.J., 1981, MNRAS 196,101
Caplan J., Deharveng L., 1985, A&AS 62, 63
Caplan J., Deharveng L., 1986, A&A 155, 297
Cassatella A., Barbero J., Brocato E., et al., 1996, A&A 306, 125
Conti P.S., Leep E.M., 1974, ApJ 193, 113
Conti P.S., Underhill A.B., 1988, Monograph Series "O stars and Wolf-Rayet Stars", NASA
Comerón F., 1997, A&A 326, 1195
Chin Y.-N., Henkel C., Whiteoak J.B., et al., 1997, A&A 317, 548
Chu, Y-H., 1982, ApJ 254, 578
Chu Y.H., 1991, in: Van Der Hucht K.A. and Hidayan B. (eds.) IAU Symp. No. 143, WR stars and interrelation with other massive stars in galaxies, p. 349
Chu, Y-H., 1997, private communication
Davies R.D., Elliot K.M., Meaburn J., 1976, MNRAS 81, 89
Dopita M.A., Bell J.F., Chu Y.-M., Lozinskaya T.A., 1994, ApJS 93, 455
Dyson J.E., Williams D.A., 1980, "The Physics of the Interstellar Medium" Manchester Univ. Press.
Epchtein N., Braz M.A., Sèvre F., 1984, A&A 140, 67
Feast M.W., 1991, In the Magellanic Clounds, IAU symposium, No. 148, p. 1
Freeman et al., 1983, ApJ 272,488
García-Segura G., Langer N. and Mac Low M., 1996a, A&A 316, 133
García-Segura G., Mac Low M.M., Langer N., 1996b, A&A 305, 229
Garnett D.J. and Chu Y-H., 1994, PASP 106, 626
Haynes R.F., Caswell J.L., 1981, MNRAS 197, 23
Henize K.G., 1956, ApJS 2, 315
Israel F.P., Johansson L.E.B., Lequeux J. et al., 1993, A&A 276, 25
Koesterke L., Hamann W.R., Schmutz W., Wessolowski U., 1991, A&A 248,166
Lamers H.J.G.L.M., 1981, ApJ 245, 593
Lucke P.B., Hodge P.W., 1970, AJ 75, 171
Madore B.F., Freeman W.L., 1998, ApJ 492, 110
Marston A.P., Chu Y-H and García-Segura G., 1994a, ApJS 93, 229
Marston A.P., Yocum D.R., García-Segura G. and Chu Y-H., 1994b, ApJS 95, 151
Marston A.P., 1995a, AJ 109, 1839
Marston A.P., 1995b, AJ 109, 2257
McGee R.X., Brooks J.W., Batchelor R.A., 1972, Aust. J. Phys. 25, 581
McGee R.X., Newton L.M., Brooks J.W., 1974, Aust. J. Phys., 27, 729
Milne D.K., Caswell J.L. and Haynes R.F., 1980, MNRAS 191, 469
Morgan D.H. and Good A.R., 1985, MNRAS 216, 459
Morton D.C., 1967, ApJ 150, 535
Oey, M.S., 1996, ApJ 467, 666
Panagia N.,1973, AJ 78, 929
Panagia N., Gilmozzi R., Adorf H-M et al., 1991, ApJ 380, L23
Rohlfs K., Kreitschmann J., Siegman B.C., Feitzinger J. V., 1984, A&A 137, 343
Rosado M., 1984, Université de Paris VII, thesis
Rosado M., 1986, A&A 160, 211
Rosado M., Laval A., Le Coarer E., et al., 1996, A&A 308, 588
Rosado M., Laval A., Le Coarer E., et al., 1998, A&A 329, 631
Santos J.F.C. Jr., Bica E., Claria J.J. et al., 1995, MNRAS 276, 1155
Scalise E. Jr., Braz M.A., 1982, AJ 87, 528
Schaerer D., Meynet G., Maeder A., Schaller G., 1993, A&AS 98, 523
Schmidt-Kaler Th., 1983, Landolt-Bornstein, New series, Group VI, vol. 23 (Springer) p.14
Smith A.M., 1970, ApJ 160, 595
Smith A.M., Cornet R.H., Hill R.S., 1987, ApJ 320, 609
Vacca W.D., Garmany C.D., Shull J.M., 1996, ApJ 460, 914
Vallenari A., Aparicio A., Fogotto F. et al., 1994, A&A 284, 447
Van Buren D., 1986, ApJ 306, 538
Walborn N.R., 1977, ApJ 215, 53
Walborn N.R., Lennon D.J., Haser S.M. et al., 1995, PASP 107, 104
Wang Q., Helfand D.J., 1991, ApJ 373, 497
Weaver R., Mc Cray R., Castor J. et al., 1977, ApJ 218, 377
Weis K, Chu Y.H., Duschl W.J., Bomans D.J., 1997, A&A 325, 1157
Whiteoak J.B., Wellington K.J., Jauncey D.L. et al., 1983, MNRAS 205, 275
Yorke H.W., Bodenheimer P., Tenorio-Tagle G., 1982, A&A 108, 25